P3.11 EFFECTS OF ALONG-TRACK INTEGRATION ON DOPPLER VELOCITY BIAS WITH A SPACEBORNE CLOUD-PROFILING RADAR

Akihisa Uematsu[1]*, Yuichi Ohno[1], Hiroaki Horie[1,2], Hiroshi Kumagai[1], and Nick Schutgens[3]
[1] National Institute of Information and Communications Technology, Koganei, Tokyo, Japan
[2] Japan Aerospace Exploration Agency, Tsukuba, Ibaraki, Japan
[3] Center for Climate System Research, University of Tokyo, Kashiwa, Chiba, Japan

1. INTRODUCTION

Measurement of vertical velocity of clouds is important to evaluate falling velocity of cirrus ice crystal, to evaluate falling velocity of water clouds (stratus, stratocumulus, etc.) for identification of drizzle, and to detect updrafts inside convective clouds. CloudSat (Stephens et al. 2002) is the first spaceborne cloud-profiling radar, and followed by CloudSat, EarthCARE (Earth Cloud, Aerosol, and Radiation Explorer) CPR (Cloud-Profiling Radar) is planned to be the first to make measurement of Doppler velocity of clouds from space (Battrick 2004).

Concept of Doppler velocity measurement from space was proposed for rain measurement (Meneghini and Kozu 1990; Amayenc et al. 1993). For spaceborne Doppler radar, if distribution of cloud and precipitation within radar beam is not uniform (NUBF; Non-Uniform Beam Filling), observed Doppler velocity has bias and sometimes aliasing is caused. Evaluation of Doppler velocity bias has been performed (Tanelli et al. 2002; Schutgens 2007). Especially, Doppler velocity bias induced by NUBF is almost proportional to horizontal gradient of radar reflectivity (Tanelli et al. 2002; Schutgens 2007). Furthermore, based on FFT method, Tanelli et al. (2004) proposed correction algorithm using Doppler spectrum data.

* *Corresponding author address:* Akihisa Uematsu, National Institute of Information and Communications Technology, 4-2-1 Nukui-kitamachi, Koganei, Tokyo, 184-8795 Japan; e-mail: uematsu@nict.go.jp

For EarthCARE CPR, pulse-pair operation will be used for measurement of Doppler velocity. Data will be horizontally integrated over 500 m-10 km in order to reduce random error and to improve accuracy. However, effects of along-track integration on NUBF-induced Doppler velocity bias over long distance (~10 km) have not been discussed. In this study, effects of along-track integration on Doppler velocity bias induced by NUBF and smoothing are evaluated.

2. DOPPLER VELOCITY BIAS INDUCED BY NON-UNIFORM BEAM FILLING (NUBF)

For pulse-pair operation, Doppler velocity is calculated from covariance of complex received power Z of consecutive two pulses. Ensemble average of covariance $R(T_s)$ is given by (Doviak and Zrnic 1993)

$$R(T_s) = \left\langle Z_t^* Z_{t+T_s} \right\rangle = \frac{G^2 \lambda^2 P_t}{(4\pi)^3} \int_V \left[\frac{f^2(\theta') W^2}{l^2 r^4} \eta \times \exp\left\{ -8\left(\frac{\pi \sigma_v T_s}{\lambda} \right)^2 \right\} \exp\left\{ -j\left(\frac{4\pi v T_s}{\lambda} \right) \right\} \right] dV \quad (1)$$

where G is the radar power gain, λ wavelength of the radar, P_t transmitted power, W range weighting function, l one-way attenuation loss, σ_v velocity width, which are regarded as constant in this paper. $f(\theta)$ is the normalized one-way power gain of the radiation pattern, θ angle, r range, and T_s pulse repetition period. η is backscatter coefficient of clouds, and v vertical velocity of clouds. Doppler velocity is calculated by (Doviak and Zrnic

1993)

Table 1: Specification of EarthCARE CPR

Frequency	94.05 GHz
Antenna aperture	2.5 m
Beam width	0.09°
Peak transmission power	1.5 kW
Pulse width	3.3 μs
PRF	> 6100 Hz (variable)
Minimum reflectivity	−35 dBZ

$$V = -\frac{\lambda}{4\pi T_s}\tan^{-1}\frac{\sum\left[\mathrm{Im}\{R(T_s)\}\right]}{\sum\left[\mathrm{Re}\{R(T_s)\}\right]}. \qquad (2)$$

As shown in Equation (2), Doppler velocity is calculated from ratio between along-track average of real and imaginary parts of covariance $R(T_s)$. Real and imaginary parts of $R(T_s)$ along horizontal integration of 500 m are calculated onboard satellite. On the ground, integration of 500 *n* meters (*n* is integer; 1 km, 2 km, 5 km, 10 km, etc.) can also be calculated.

Schutgens (2007) evaluated both random error and bias with considering random stochastic variation of received power. The aim of this study is to evaluate effects of horizontal integration on Doppler velocity bias. We checked that without considering random stochastic variation, the same velocity bias can be obtained. We also ignored effects of signal-to-noise ratio.

Table 1 shows specification of EarthCARE CPR. EarthCARE CPR is nadir-pointing spaceborne radar with pulse-pair operation. Minimum reflectivity is −35 dBZ, which is 7 dBZ more sensitive than that of CloudSat. Beam width is 0.09° and instantaneous field of view (IFOV) is 700 m. Figure 1 shows schematic figure of Doppler velocity observation with CPR. In this paper, altitude of satellite is 440 km, pulse repetition period is 150 μs (pulse repetition frequency 6667 Hz), satellite speed is 7.65 km s^{-1} and velocity of sub-satellite point is 7.15 km s^{-1}. Ground track of 500 m corresponds to integration over 465 pulses.

3. SIMULATION WITH SIMPLIFIED CLOUD SCENE

3.1 *A case with variable reflectivity and constant velocity*

Doppler velocity bias with constant velocity and variable reflectivity is first evaluated. Figure 2 shows results with varied relative reflectivity (0-10 dB) and no vertical velocity (0 m s^{-1}, constant) with horizontal integration of 500 m, 1 km, 2 km, 5 km, and 10 km. As shown in Figure 2a, scene is changed at horizontal axis x = −5 and 5 km and constant gradient within 700 m (same as IFOV; also the same in Figure 3). Figures 2b and c show simulated reflectivity and velocity, respectively. Positive (negative) Doppler velocity indicates upward (downward) velocity.

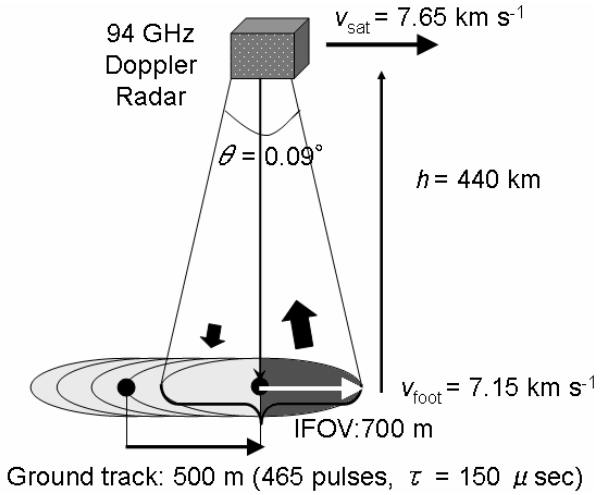

Figure 1: Schematic figure of Doppler velocity observation with spaceborne CPR.

At x = −5 km and 5 km, upward and downward velocity are found, respectively. This corresponds to radar approaching to and leaving from large reflectivity area (10 dB). If distance of horizontal integration is larger, Doppler velocity bias is smaller; however, peak of the bias is shifted.

3.2 *A case with variable reflectivity and variable velocity*

In general, radar reflectivity and particle falling speed is related. Figure 3 shows results with variable reflectivity (0-10 dB) and variable velocity (0- −3 m s^{-1}) assuming precipitation between cloudy areas (Figures 3a and b). Figures 3c and d are simulated reflectivity and velocity, respectively. Around x = −5 km (corresponding to the front of precipitation), simulated velocity is positive indicating unrealistic updraft. If distance of horizontal integration gets larger (5-10 km), such upward bias is smaller; however, region of downward

velocity (corresponds to falling rain drops) is larger. This indicates that precipitation region is overestimated especially for 10 km integration.

Around x = 5 km (corresponding to the rear of precipitation), aliasing occurs with horizontal integration of 500 m-2 km, and this aliasing does not return (inverse aliasing does not occur) before vertical velocity becomes 0 m s^{-1}. Therefore it implies that if distance of horizontal integration is short, correction of aliasing at the rear of precipitation boundary is difficult. With horizontal integration of 5 km and 10 km, such aliasing does not occur. This shows that to avoid aliasing at cloud boundary, usage of longer integration distance is effective.

4. SIMULATION WITH REALISTIC CLOUD SCENE

Evaluation of Doppler velocity bias is also performed based on ground-based observation of clouds with a 95-GHz radar (SPIDER; Horie et al. 2000). Data obtained at 26 June 2006 is used. Original time-height data is converted to distance-height data under assumption of constant horizontal wind with 20 m s^{-1}. Two patterns of horizontal integration, 500 m (Figures 4-5) and 10 km (Figures 6-7), are simulated.

Doppler velocity bias can be divided into two factors: 1) smoothing bias due to averaging over 500 m-10 km, and 2) NUBF-induced bias due to large satellite speeds (v_s = 7.65 km s^{-1}). To separate these two factors, following two patterns are simulated: 1) velocity with no satellite speeds and only smoothing effect is included (Figures 4e and 6e), and 2) velocity with satellite speeds v_s = 7.65 km s^{-1} and both smoothing and NUBF-induced bias are included (Figures 4f and 6f).

4.1 *Horizontal integration of 500 m*

Figure 4a shows original radar reflectivity for simulation. Figure 4b is simulated radar reflectivity, and Figure 4c is horizontal gradient of simulated reflectivity. Oblique pattern of both reflectivity and reflectivity gradient are found corresponding to falling cloud particle. Figure 4d is original vertical velocity of cloud. Downward motion due to falling cloud particle is dominant at lower part of stratiform cloud.

Figures 4e and 4f shows simulated Doppler velocity with satellite speeds v_s = 0 and 7.65 km s^{-1}, respectively. In Figure 4f, Doppler velocity is biased and similar pattern to reflectivity gradient (Figure 4c) is found, as discussed by Tanelli et al. (2002).

Difference between simulated and original vertical velocity is also computed. Figure 4g is bias due to smoothing (difference between Figures 4d and 4e). Figure 4h is bias induced by NUBF with large satellite speeds (difference between Figures 4e and 4f), and Figure 4i is total velocity bias (difference between Figures 4d and 4f). Compared to smoothing bias (Figure 4g) and NUBF bias (Figure 4h), smoothing bias is smaller, and therefore NUBF bias is quite dominant for total velocity bias. Total velocity bias (Figure 4i) has almost the same pattern as NUBF bias (Figure 4h).

Figure 5a shows scatter plot between horizontal gradient of radar reflectivity (Figure 4c) and NUBF bias (Figure 4h). In most data, linear relationship exists between horizontal gradient of radar reflectivity and velocity bias, as discussed in Tanelli et al. (2002) and Schutgens (2007). A few data has large bias due to aliasing. Figure 5b shows scatter plot between reflectivity gradient (Figure 4c) and total velocity bias (Figure 4i). Since Figures 4h and 4i have similar pattern, results between Figures 5a and 5b are also similar.

According to linear approximation of relationship based on Figure 5a, reflectivity gradient of 1 dBZ km^{-1} corresponds to velocity bias of 0.218 m s^{-1}. Using this relation, Doppler velocity is corrected as shown in Figure 4j. Pattern of Doppler velocity bias related to reflectivity gradient disappears well. Standard deviation of residual bias after correction is 0.254 m s^{-1}. That of total velocity bias before correction is 0.375 m s^{-1}; therefore, velocity bias is reduced by correction.

4.2 *Horizontal integration of 10 km*

Figure 6 shows result with horizontal integration of 10 km. Simulated reflectivity (Figure 6b) and velocity (Figure 6e and 6f) are smoothed. Compared to Figures 4c and 6c, reflectivity gradient is quite smaller in 10 km integration. Smoothing bias is larger (Figure 6g), while NUBF bias is smaller (Figure 6h). Pattern of total velocity bias (Figure 6i) is similar to

smoothing bias (Figure 6g). Standard deviation of total velocity bias is 0.268 m s^{-1}, while that of bias induced by NUBF only is 0.086 m s^{-1}.

Figure 7 shows scatter plot for 10 km integration. Relation between reflectivity gradient and velocity bias can be approximated linearly as well as 500 m integration (Figure 5a). Reflectivity gradient of 1 dBZ km^{-1} corresponds to 0.163 m s^{-1}. Figure 7b has almost the same linear relation; however, dispersion of data is larger because effect of smoothing is included.

Corrected Doppler velocity is shown in Figure 6j by using relationship in Figure 7a. Downward velocity at the lower part of stratiform cloud is well represented also with 10 km integration. Residual velocity bias due to NUBF is much reduced (standard deviation is 0.034 m s^{-1}). This indicates that in the case of 10 km integration effects of NUBF-induced bias on corrected Doppler velocity is small. However, residual bias of both smoothing and NUBF is still 0.254 m s^{-1}, because smoothing bias is dominant for 10 km integration.

5. SUMMARY

Doppler velocity bias induced by NUBF and smoothing are evaluated for EarthCARE spaceborne cloud-profiling Doppler radar. Especially, effects of horizontal integration (500 m-10 km) on velocity bias, and possibility of correction based on reflectivity gradient for 500 m and 10 km integration is discussed. Utilization of reflectivity gradient is effective for both 500 m and 10 km integration, and for 10 km integration, NUBF-induced bias is small.

In this study, only one stratiform cloud case was simulated for realistic cloud scene. Simulation of convective and precipitating cloud is also planned.

REFERENCES

Amayenc, P., J. Testud, and M. Marzoug, 1993: Proposal for a spaceborne dual-beam rain radar with Doppler capability. *J. Atmos. Oceanic Technol.*, 10, 262-276.

Battrick, B., Eds., 2004: *EarthCARE – Earth Clouds, Aerosols and Radiation Explorer.* ESA Publications Division, 60 pp.

Doviak, R. J., and D. S. Zrnic, 1993: *Doppler Radar and Weather Observations.* Academic Press, 562 pp.

Horie, H., T. Iguchi, H. Hanado, H. Kuroiwa, H. Okamoto, and H. Kumagai, 2000: Development of a 95-GHz airborne cloud profiling radar (SPIDER) - Technical aspects-. *IEICE Trans. Commun.*, E83-B, 2010-2020.

Kobayashi, S., H. Kumagai, and T. Iguchi, 2003: Accuracy evaluation of Doppler velocity on a spaceborne weather radar through a random signal simulation. *J. Atmos. Oceanic Technol.*, 20, 944-949.

Meneghini, R. and T. Kozu, 1990: *Spaceborne Weather Radar.* Artech House, 201 pp.

Schutgens, N. A. J., 2007: Simulated Doppler radar observations of inhomogeneous clouds; application to the EarthCARE space mission, *J. Atmos. Oceanic Technol.*, in press.

Stephens, G. L., D. G. Vane, R. J. Boain, G. G. Mace, K. Sassen, Z. Wang, A. J. Illingworth, E. J. O'Connor, W. B. Rossow, S. L. Durden, S. D. Miller, R. T. Austin, A. Benedetti, C. Mitrescu, and CloudSat Science Team, 2002: The CloudSat mission and the A-train, *Bull. Amer. Meteor. Soc.*, 83, 1771-1790.

Tanelli, S., E. Im, S. L. Durden, L. Facheris, and D. Giuli, 2002: The effects of nonuniform beam filling on vertical rainfall velocity measurements with a spaceborne Doppler radar, *J. Atmos. Oceanic Technol.*, 19, 1019-1034.

Tanelli, S., E. Im, S. L. Durden, L. Facheris, D. Giuli, and E. A. Smith, 2004: Rainfall Doppler velocity measurements from spaceborne radar: overcoming nonuniform beam-filling effects, *J. Atmos. Oceanic Technol.*, 21, 27-44.

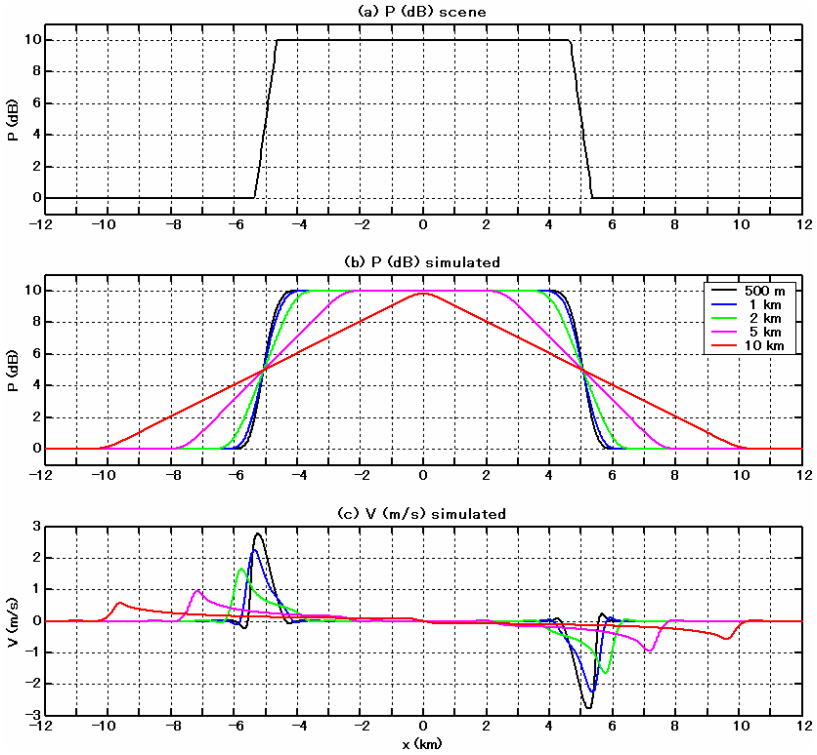

Figure 2: (a) Relative reflectivity of original cloud scene. (b) Simulated relative reflectivity. (c) Simulated Doppler velocity. Original vertical velocity is 0 m s^{-1} (constant). Distances of horizontal integration are 500 m, 1 km, 2 km, 5 km, and 10 km.

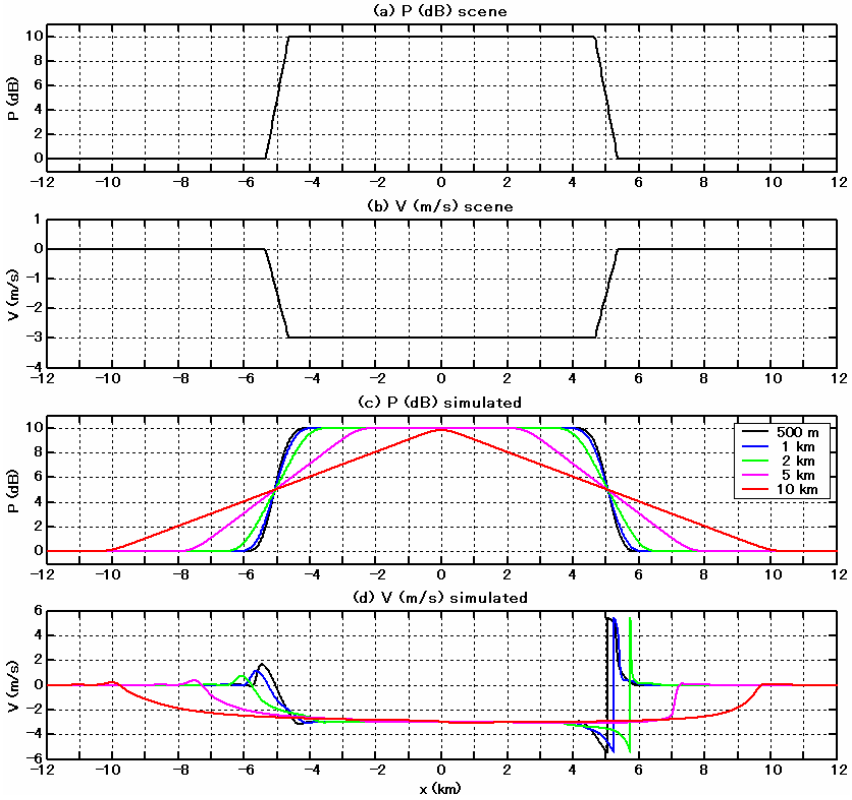

Figure 3: (a) Relative reflectivity of original cloud scene. (b) Vertical velocity of original cloud scene. (c) Simulated relative reflectivity. (d) Simulated Doppler velocity. Distances of horizontal integration are 500 m, 1 km, 2 km, 5 km, and 10 km.

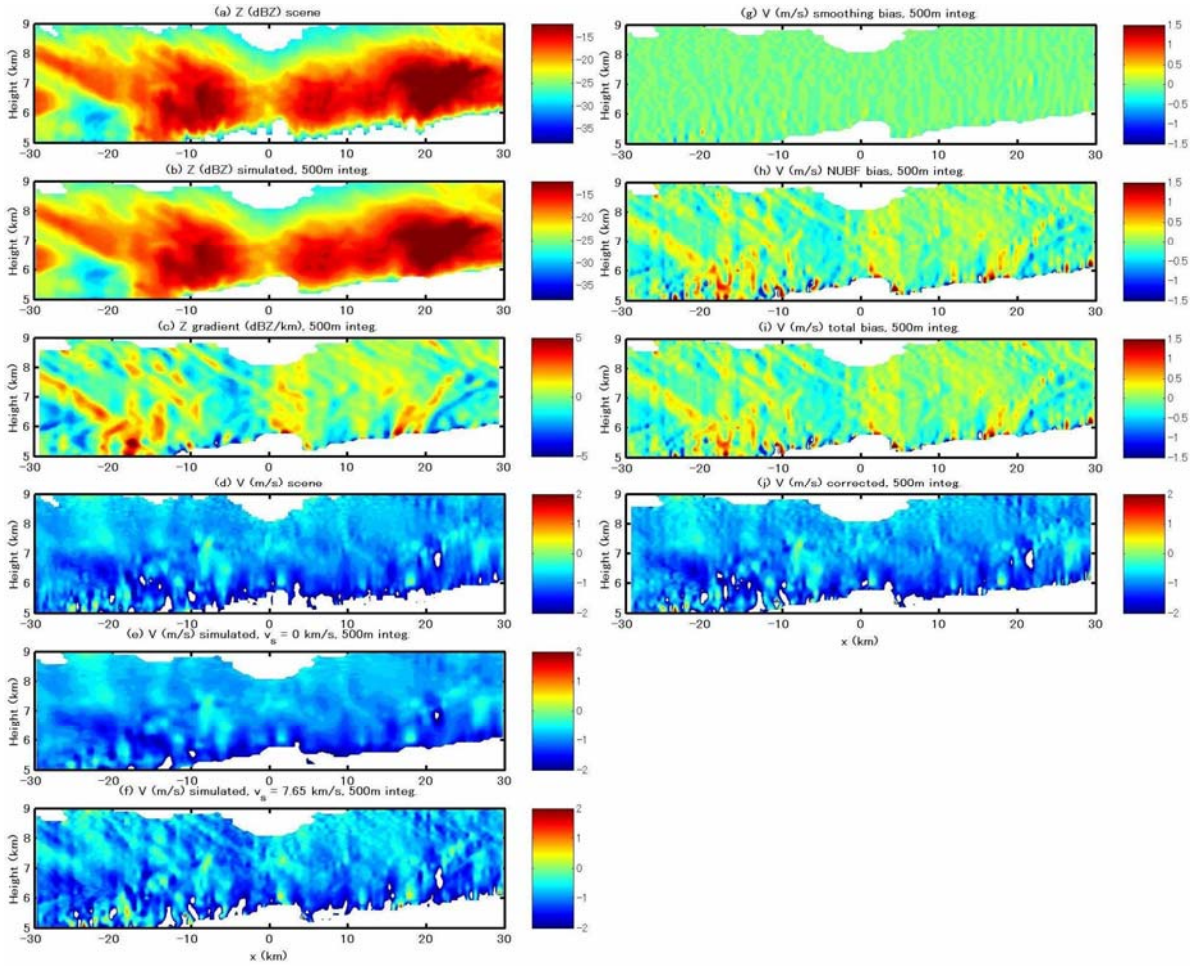

Figure 4: (a) Original radar reflectivity of cloud. (b) Simulated radar reflectivity for horizontal integration of 500 m. (c) Horizontal gradient of simulated radar reflectivity. (d) Same as (a) but for vertical velocity. (e) Simulated Doppler velocity with no satellite speeds. (f) Simulated Doppler velocity with satellite speeds v_s = 7.65 km s^{-1}. (g) Doppler velocity bias due to smoothing. (h) Doppler velocity bias due to NUBF and large satellite speeds. (i) Total Doppler velocity bias. (j) Corrected Doppler velocity using relationship between reflectivity gradient and Doppler velocity bias.

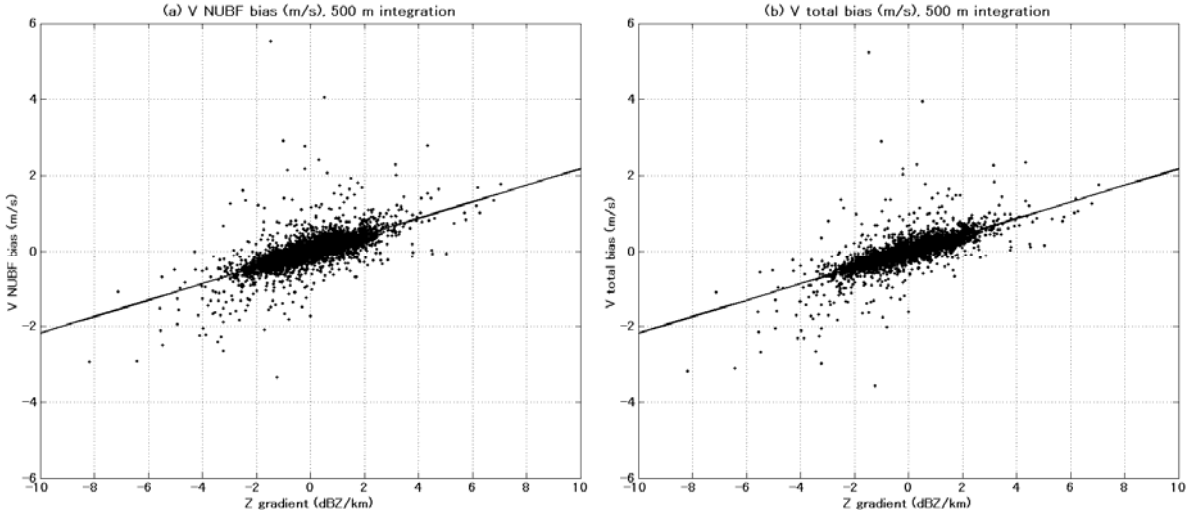

Figure 5: (a) Scatter plot between horizontal gradient of radar reflectivity and velocity bias due to NUBF for 500 m integration. (b) Scatter plot between horizontal gradient of radar reflectivity and total velocity bias.

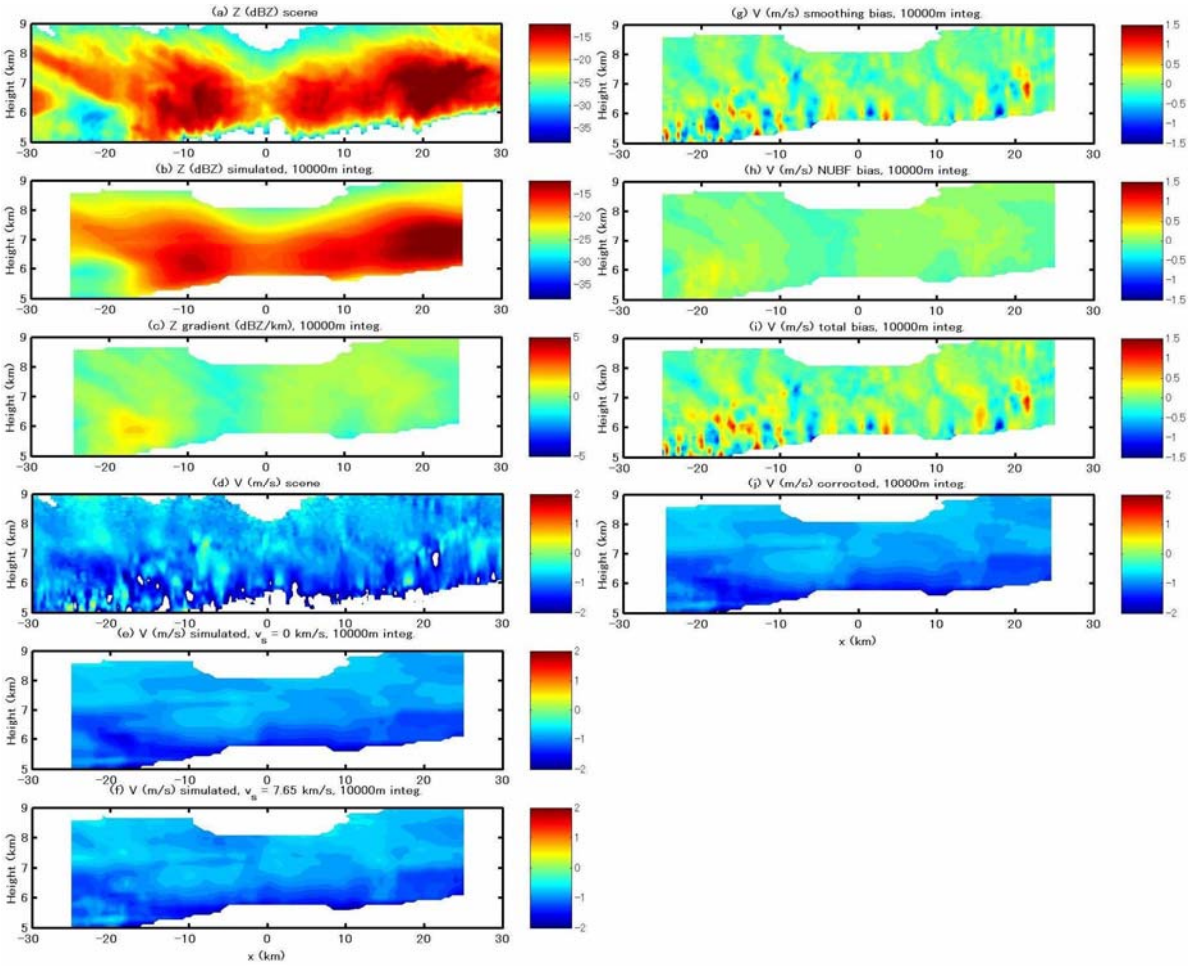

Figure 6: Same as Figure 4 but for horizontal integration of 10 km.

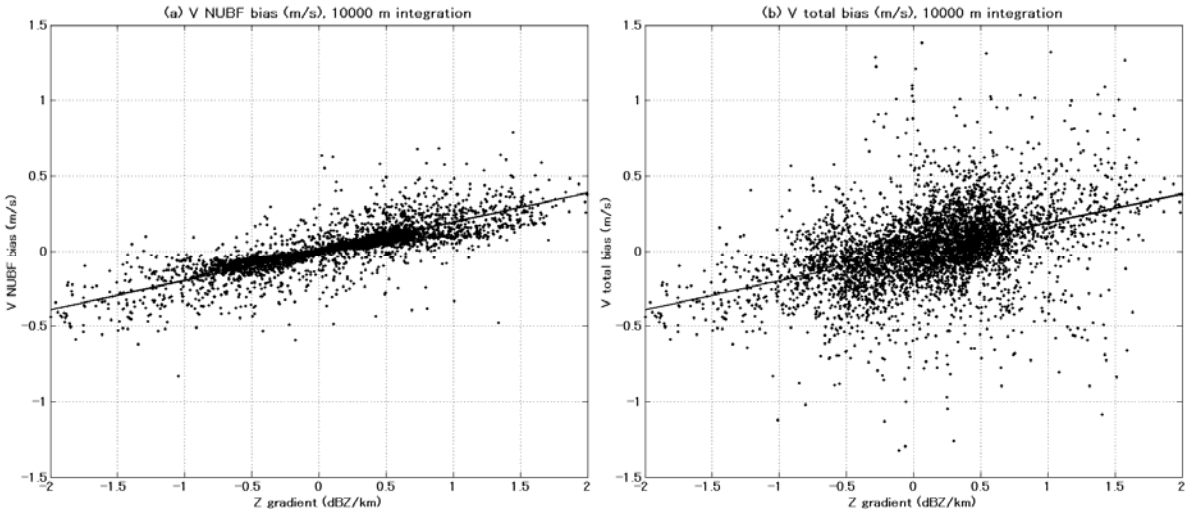

Figure 7: Same as Figure 5 but for 10 km integration.